Radiology

Gadolinium Deposition in Human Brain Tissues after Contrast-enhanced MR Imaging in Adult Patients without Intracranial Abnormalities[1]

Robert J. McDonald, MD, PhD
Jennifer S. McDonald, PhD
David F. Kallmes, MD
Mark E. Jentoft, MD
Michael A. Paolini, MD
David L. Murray, MD, PhD
Eric E. Williamson, MD
Laurence J. Eckel, MD

Purpose: To determine whether gadolinium deposits in neural tissues of patients with intracranial abnormalities following intravenous gadolinium-based contrast agent (GBCA) exposure might be related to blood-brain barrier integrity by studying adult patients with normal brain pathologic characteristics.

Materials and Methods: After obtaining antemortem consent and institutional review board approval, the authors compared postmortem neuronal tissue samples from five patients who had undergone four to 18 gadolinium-enhanced magnetic resonance (MR) examinations between 2005 and 2014 (contrast group) with samples from 10 gadolinium-naive patients who had undergone at least one MR examination during their lifetime (control group). All patients in the contrast group had received gadodiamide. Neuronal tissues from the dentate nuclei, pons, globus pallidus, and thalamus were harvested and analyzed with inductively coupled plasma mass spectrometry (ICP-MS), transmission electron microscopy with energy-dispersive x-ray spectroscopy, and light microscopy to quantify, localize, and assess the effects of gadolinium deposition.

Results: Tissues from the four neuroanatomic regions of gadodiamide-exposed patients contained 0.1–19.4 μg of gadolinium per gram of tissue in a statistically significant dose-dependent relationship (globus pallidus: $\rho = 0.90$, $P = .04$). In contradistinction, patients in the control group had undetectable levels of gadolinium with ICP-MS. All patients had normal brain pathologic characteristics at autopsy. Three patients in the contrast group had borderline renal function (estimated glomerular filtration rate <45 mL/min/1.73 m^2) and hepatobiliary dysfunction at MR examination. Gadolinium deposition in the contrast group was localized to the capillary endothelium and neuronal interstitium and, in two cases, within the nucleus of the cell.

Conclusion: Gadolinium deposition in neural tissues after GBCA administration occurs in the absence of intracranial abnormalities that might affect the permeability of the blood-brain barrier. These findings challenge current understanding of the biodistribution of these contrast agents and their safety.

[1] From the Departments of Radiology (R.J.M., J.S.M., D.F.K., E.E.W., L.J.E.), Neurosurgery (D.F.K.), and Laboratory Medicine and Pathology (M.E.J., M.A.P., D.L.M.), College of Medicine, Mayo Clinic, 200 1st St SW, Rochester, MN 55905. Received July 24, 2016; revision requested October 17; revision received March 8, 2017; accepted March 20; final version accepted March 27. **Address correspondence to** R.J.M. (e-mail: *mcdonald.robert@mayo.edu*).

Emerging evidence of intracranial gadolinium deposits after intravenous administration of gadolinium-based contrast agents (GBCAs) for routine magnetic resonance (MR) imaging has raised serious concerns about the safety of these contrast agents. Kanda and colleagues (1) initially reported the positive correlation between increased signal intensity in the dentate nucleus and basal ganglia and previous exposure to GBCAs. Subsequent studies directly confirmed the presence of gadolinium deposits within neuronal tissues and a dose-dependent relationship with cumulative GBCA exposure (2–4). Despite the small sample sizes, these studies suggested that gadolinium tissue deposition was taking place in the setting of normal renal function and that these deposits may remain in tissues for months to years after exposure to intravenous GBCAs.

In our previous study using electron microscopy (3), we were able to localize and quantify the distribution of these deposits within the neural tissues. In that analysis, we discovered that a majority of the gadolinium deposits were sequestered within the endothelial walls, presumably trapped behind the tight junction of the blood-brain barrier, and a minority of deposits were scattered throughout the neural interstitium. This latter finding is surprising and suggests that some chemical species of gadolinium (free or chelated) are capable of either directly or indirectly circumventing an apparently intact blood-brain barrier. Because most patients in these recent studies had underlying intracranial abnormalities, it is possible that the underlying intracranial lesion or treatment could have injured the surrounding tissues, thereby damaging the blood-brain barrier and rendering it more permeable to larger molecules such as GBCAs. If true, this theory would suggest that the phenomenon of gadolinium tissue deposition is entirely limited to patients with intracranial abnormalities. Alternatively, if intracranial gadolinium deposits were discovered in patients with normal brain pathologic features, it would suggest that this phenomenon is more widespread than currently assumed, occurring by means of an undefined mechanism of deposition and potentially affecting tens of millions of patients worldwide.

In the current study, we sought to examine the phenomenon of intracranial gadolinium deposition in patients lacking intracranial abnormalities who underwent multiple gadolinium-enhanced MR examinations.

Advances in Knowledge

- Elemental gadolinium accumulates in neuronal tissues after intravenous administration of a gadolinium-based contrast agent (GBCA) in the absence of intracranial abnormalities.
- Inductively coupled plasma mass spectrometry of autopsied brains exposed to GBCAs demonstrates a significant dose-dependent relationship in the amount of gadolinium deposited within neuronal tissues (Spearman rank correlation coefficient [ρ] = 0.82–0.94, $P < .04$).
- Gadolinium deposition occurs in all sampled sites (globus pallidus, thalamus, dentate, pons) and is greatest in the dentate nucleus, with concentrations of 0.1–19.4 μg of gadolinium per gram of tissue.
- Findings from transmission electron microscopy suggest that a majority of detectable gadolinium deposits occurs within the endothelial walls and a smaller fraction of deposits is detected in the interstitium, some within the cytoplasm and nucleus of neurons within the dentate nuclei.

Implications for Patient Care

- Neuronal tissue deposition of gadolinium appears to be cumulative during a patient's lifetime and occurs in the absence of intracranial abnormalities that could potentially weaken the blood-brain barrier.
- Neuronal tissue deposition appears to take place in all patients exposed to gadolinium and is detectable with as few as four lifetime doses of GBCA.
- The presence of gadolinium deposits within the cytoplasm of neurons, particularly within the nucleus, raises the possibility of biologic activity of these deposits, possibly from modulation of calcium channel activity or direct interaction with cellular biomolecules; these facts notwithstanding, the clinical significance of gadolinium deposition in neural tissues remains undefined without evidence of neurotoxicity at this time.

Materials and Methods

The design and execution of this single-center retrospective study were subject to institutional review board oversight and Health Insurance Portability and Accountability Act guidelines regarding patient data integrity and privacy.

Study Design and Population

Deceased adult patients (≥18 years) in whom autopsy was performed following antemortem consent and who had

https://doi.org/10.1148/radiol.2017161595

Content code: NR

Radiology 2017; 285:546–554

Abbreviations:
GBCA = gadolinium-based contrast agent
ICP-MS = inductively coupled plasma mass spectrometry

Author contributions:
Guarantors of integrity of entire study, R.J.M., J.S.M.; study concepts/study design or data acquisition or data analysis/interpretation, all authors; manuscript drafting or manuscript revision for important intellectual content, all authors; manuscript final version approval, all authors; agrees to ensure any questions related to the work are appropriately resolved, all authors; literature research, R.J.M., J.S.M., M.E.J., D.L.M., L.J.E.; clinical studies, R.J.M., J.S.M., E.E.W., L.J.E.; experimental studies, M.E.J., M.A.P., D.L.M.; statistical analysis, R.J.M.; and manuscript editing, R.J.M., J.S.M., D.F.K., M.E.J., D.L.M., E.E.W., L.J.E.

Conflicts of interest are listed at the end of this article.

See also the editorial by Kang and the article by McDonald et al in this issue.

undergone at least one unenhanced MR examination (control group) or at least four gadolinium-enhanced MR examinations (contrast group) of the chest, abdomen, pelvis, and/or extremities at our institution from 2000 to 2014 were included in this study. Pediatric patients (<18 years, both groups) and those with intracranial disease that could potentially alter the permeability of the blood-brain barrier (known at or before the time of autopsy, contrast group only) were excluded from further study. The control group consisted of adult patients (>18 years) who had undergone at least one unenhanced MR examination of the brain (3). All clinical and procedural data were extracted from our institutional electronic medical record system by R.J.M. (6 years of experience) and J.S.M. (7 years of experience) with use of relational database software (Data Discovery and Query Building; IBM, Armonk, NY) as previously described (3).

MR Imaging and GBCA Administration

All patients in this study underwent MR examination of the chest, abdomen, pelvis, or extremities with one of 10 MR imaging systems at our institution dedicated to thoracic, abdominal, breast, or musculoskeletal imaging (five GE 1.5-T units [GE Healthcare; Little Chalfont, England], two GE 3.0-T units, two Siemens 1.5-T units [Siemens Healthcare; Erlangen, Germany], and one Siemens 3.0-T unit). All gadolinium-enhanced MR examinations were performed with the intravenous agent gadodiamide (Omniscan, GE Healthcare) by using an institutional weight-based nomogram for a target dose of 0.1 mmol/kg. Renal function was assessed before each MR examination to screen for chronic renal failure by using estimated glomerular filtration rate derived from serum creatinine results collected within 24 hours of the examination (5).

Tissue Processing

All autopsies and brain sectioning were performed by one of three board-certified staff neuropathologists (including M.E.J.) with 10–37 years of experience, as previously described (3). In brief, tissue samples were harvested from the posterior fossa (dentate nucleus and pons) and basal ganglia (globus pallidus and thalamus) of archived formalin-fixed whole-brain specimens. Whole-brain specimens were removed at the time of autopsy, fixed in formalin for approximately 10 days, sectioned into approximately 0.5-cm-thick samples, placed in 10% neutral buffered formalin, and archived in our institutional biospecimen repository. Tissue samples for this study were harvested from the posterior fossa (dentate nucleus and pons) and basal ganglia (globus pallidus and thalamus) of archived whole-brain specimens and placed in formalin solution for further analysis. Autopsy records were reviewed in conjunction with inspection of the sectioned brain to exclude the presence of underlying occult intracranial abnormalities. In addition, hematoxylin-eosin–stained microscope slides of the dentate, harvested at the time of autopsy for diagnostic purposes, were retrieved from pathology archives and reviewed (by M.E.J.).

Mass Spectrometry

Elemental gadolinium quantification of acid-hydrolyzed tissue samples was carried out by D.L.M. (20 years of experience) with use of inductively coupled plasma mass spectrometry (ICP-MS) in our institutional heavy metals laboratory as previously described (3). Briefly, desiccated formalin-fixed brain tissues were digested with a concentrated nitric acid (Fisher Scientific, Hampton, NH; 80°C, 20 minutes), quenched with hydrogen peroxide (30 wt%), and diluted with 1% nitric acid containing rhodium and terbium internal standards. Tissue gadolinium quantification was performed by using an inductively coupled plasma mass spectrometer (ELAN DRC II; Perkin Elmer, Shelton, Conn) with gadolinium masses 157 and 160. For gadolinium ions, the analytical range of this system has been shown to range from 0.1 to 1000 ng/mL. Results of tissue mass spectrometry were compared with internal standards purchased from the European Commission Joint Research Center (Geel, Belgium) and the National Institute of Standards and Technology (Gaithersburg, Md). Tissue gadolinium concentration was determined by multiplying the weight of gadolinium per milliliter in the digested solution by the dilution factor and dividing by tissue sample weight.

Transmission Electron Microscopy

Transmission electron microscopy with electron-dispersive x-ray spectroscopy was performed (R.J.M., with 14 years of experience, and another investigator with 27 years of experience) at our institutional microscopy core facility to characterize and quantify the distribution of gadolinium deposits in these formalin-fixed tissues as previously described (3). Briefly, formalin-fixed tissue samples were rinsed in 0.1 mol/L phosphate buffer, secondarily fixed in Trump fixative (4% paraformaldehyde plus 1% glutaraldehyde in 0.1 mol/L phosphate buffer), dehydrated by means of an ethanol series, and embedded in epoxy resin (Embed 812 + Araldite 502; EMS, Hatfield, Pa). Ultrathin embedded tissue slices (0.1 μm) were then stained with 2% lead citrate and mounted on platinum grids. Micrographs were acquired by using a transmission electron microscope (Technai G^2 12; FEI, Hillsboro, Ore) equipped with an energy-dispersive spectrometry system (EDAX, Mahweh, NJ). Image densitometry was performed by using image-processing software (ImageJ; National Institutes of Health, Bethesda, Md) to quantify the fraction of electron-dense foci present within the neuronal interstitium relative to the total amount detected in the image.

Statistical Analysis

All statistical analyses were performed by R.J.M. (16 years of experience) and J.S.M. (17 years of experience) with use of software (R, version 3.1; R Foundation for Statistical Computing, Vienna, Austria) (6). Continuous variables are presented as medians and interquartile ranges owing to nonnormal data distributions unless otherwise noted. Differences in the amounts of gadolinium detected in the four sampled neuronal tissues with ICP-MS were

assessed by means of the Mood median test. Correlations among cumulative gadolinium dose, changes in T1 signal intensity, and the amount of gadolinium detected in neuronal tissues with ICP-MS were assessed by using the nonparametric Spearman rank correlation (ρ). $P \leq .05$ was indicative of a statistically significant difference.

Results

Fifteen deceased patients (five from the contrast group and 10 from the control group) met all inclusion and exclusion criteria for this study. The demographic and clinical characteristics of these patients are shown in Table 1. Patients in the contrast group had undergone four to 18 separate contrast-enhanced MR examinations; the previously identified 10 control patients had no history of GBCA exposure. None of the patients in the contrast group had presented during their lifespan with neurologic symptoms that warranted intracranial MR imaging. All but one patient in the contrast group had undergone MR imaging only for surveillance of their respective intraabdominal or intrapelvic disease, as indicated in Table 1; the one notable exception was patient 1, who had undergone 17 contrast-enhanced MR examinations of the abdomen and one contrast-enhanced cardiac MR examination for the evaluation of myocardial function. All five patients in the contrast group and eight of the 10 in the control group had lived within Olmsted county and had received all of their adult health care at our medical center; the remaining two patients in the control group were regional patients, which enabled us to access their outside medical records and previous radiologic examination results. Contrast material–exposed patient 2 had undergone focused external beam radiation therapy for cholangiocarcinoma and patient 5 had undergone radioactive seed implantation for prostate adenocarcinoma; none of these patients had undergone irradiation of the neuraxis. Similarly, contrast material–exposed patient 2 was the only patient who had been treated with conventional

Table 1

Patient Demographics and Clinical Characteristics of Study Population

Group and Patient No.	Age at Death (y)	Examination Indication	No. of MR Examinations	Gadolinium Dose (mL)*	Time between MR Imaging and Death (d)	Estimated Glomerular Filtration Rate (mL/min/1.73 m²)†‡	Alkaline Phosphatase Level (U/L)†§	Aspartate Aminotransferase Level (U/L)†§	Total Bilirubin Level (mg/dL)†§
Contrast group									
1	73	Carcinoid tumor	18	421	1658–56	38 (36–41)	144 (129–183)	40 (28–48)	0.6 (0.5–0.7)
2	63	Cholangiocarcinoma	16	244	1153–53	104 (104–122)	201 (168–266)	34 (29–49)	0.5 (0.3–0.9)
3	71	RCC	5	109	2384–1257	24 (15–32)	150 (114–219)	54 (34–67)	7.6 (4.3–9.5)
4	68	Prostate cancer	5	100	463–1	57 (57–73)	NP	NP	NP
5	47	HCC	4	76	678–333	41 (34–45)	196 (181–270)	37 (31–55)	1.0 (0.7–1.3)
Control group									
1	84	TBI	1	…	3189	47 (47–47)	136 (78–298)	38 (27–86)	1.2 (0.5–2.0)
2	86	Dementia	2	…	3	62 (59–65)	190 (118–474)	60 (27–548)	0.5 (0.3–2.7)
3	62	Lymphoma	1	…	516	44 (41–49)	113 (95–155)	30 (19–85)	0.2 (0.1–0.2)
4	91	TIA	1	…	2	64 (51–72)	85 (71–544)	25 (14–62)	0.6 (0.5–3.0)
5	74	Dementia	1	…	791	40 (34–60)	66 (59–85)	18 (16–19)	0.7 (0.6–0.8)
6	56	Seizure	3	…	663	10 (8–11)	173 (109–457)	39 (20–87)	0.7 (0.3–1.2)
7	83	TIA	6	…	2032	62 (53–70)	103 (75–373)	41 (24–107)	0.7 (0.4–1.0)
8	92	Hydrocephalus	1	…	5008	43 (43–43)	150 (99–643)	21 (14–146)	0.6 (0.6–0.6)
9	89	Lymphoma	1	…	8	29 (18–37)	50 (38–72)	18 (18–18)	0.1 (0.1–0.1)
10	60	ICH	1	…	2359	104 (81–109)	62 (62–62)	32 (27–36)	0.7 (0.6–0.9)

Note.—HCC = hepatocellular carcinoma, ICH = intracranial hemorrhage, NP = not performed, RCC = renal cell carcinoma, TBI = traumatic brain injury, TIA = transient ischemic attack.

* Cumulative gadolinium dose from all intravenous gadolinium-enhanced MR examinations. Gadodiamide concentration = 287 mg/mL.

† Data are medians, with ranges in parentheses.

‡ Estimated glomerular filtration rate calculated by using Modification of Diet in Renal Disease equation.

§ Normal laboratory range for assays are as follows: alkaline phosphatase level, 45–142 U/L; aspartate aminotransferase level, 8–48 U/L; total bilirubin level, 0.1–1.0 mg/dL.

chemotherapy (5-fluorouracil); patient 1 had taken octeotide (Sandostatin; Novartis Pharmaceuticals, Basel, Switzerland) and soratinib for carcinoid, patient 3 had undergone nephrectomy and embolization for renal cell carcinoma, patient 4 had been treated with leuprolide (Lupron; Abbvie, North Chicago, Ill) and prostatectomy, and patient 5 had received no systemic therapy for hepatocellular carcinoma that developed after long-standing alcohol- and hepatitis C virus–induced chronic hepatitis. Control patients 3 and 9 had both undergone chemotherapy (patient 3, cyclophosphamide and dexamethasone; patient 9, cytarabine and dexamethasone); neither patient had undergone irradiation of the neuraxis. All patient medical records were reviewed; no other confounding comorbid diagnoses that may have increased the permeability of the blood-brain barrier were identified.

Patients in the contrast group underwent four to 18 contrast-enhanced MR examinations, and patients in the control group underwent one to six unenhanced MR examinations. The median age at the time of death was lower in the contrast group (68 years; range, 47–73 years) than in the control group (79 years; range, 60–88 years) (P = .27). The median time between the last MR examination and death was significantly shorter in the contrast group (56 days; range, 1–1257 days) than in the control group (727 days; range, 8–2359 days) ($P < .0001$). The median baseline renal function during MR examinations was similar among patients in the contrast group (41 mL/min/1.73 m^2; range, 24–104 mL/min/1.73 m^2) and those in the control group (46 mL/min/1.73 m^2; range, 10–104 mL/min/1.73 m^2) (P = .67). Patients 1, 3, and 5 in the contrast group had renal insufficiency throughout the course of their MR examinations, with estimated glomerular filtration rates of less than 45 mL/min/1.73 m^2. Gadolinium was withheld for one examination in patient 3 owing to poor renal function, but otherwise gadolinium was not withheld from any patient because of acute or chronic renal dysfunction. Patients 1 and 5 had an elevated aspartate aminotransferase level and patient 3 had an elevated total bilirubin level during the course of their MR examinations. Median hepatobiliary function (alkaline phosphatase, aspartate aminotransferase, and total bilirubin levels) was otherwise normal in the remaining patients in the contrast group near the time of gadolinium administration (Table 1).

Table 2

Results of Mass Spectrometry

Group and Patient No.	Dentate	Pons	Globus Pallidus	Thalamus
Contrast group				
1	8.9	0.7	19.4	2.1
2	6.7	0.2	9.0	1.1
3	2.6	0.2	11.1	0.6
4	2.2	0.7	2.1	0.9
5	6.1	0.1	3.2	0.5
Control group				
1	0	0	0	0
2	0	0	0	0
3	0	0	0	0
4	0	0	0	0
5	0	0	0	0
6	0	0	0	0
7	0	0	0	0
8	0	0	0	0
9	0	0	0	0
10	0	0	0	0

Note.—Data are gadolinium concentrations detected with ICP-MS (in micrograms of gadolinium per gram of tissue).

Effect of Gadolinium Exposure on Tissue Deposition

Elemental gadolinium was detected in the four neuroanatomic regions of all five patients in the contrast group, with concentrations ranging from 0.1 to 19.4 μg gadolinium per gram of tissue (Table 2). The highest concentration of gadolinium was detected in the globus pallidus of patients 1, 2, and 3 and in the dentate nucleus of patients 4 and 5. None of the patients in the control group had detectable levels of elemental gadolinium. For each neuroanatomic location, the cumulative gadolinium dose showed a moderate to strong correlation with tissue gadolinium concentration (Fig 1) (ρ = 0.82–0.94, $P < .04$) and followed a relatively linear correlation with linear regression (dentate: F = 10.68, R^2 = 0.73, P = .03; globus pallidus: F = 18.06, R^2 = 0.82, P = .01; thalamus: F = 69.27, R^2 = 0.95, P = .001; pons: F = 2.43, R^2 = 0.38, P = .19), despite mild to moderate chronic renal disease in several of the patients exposed to gadolinium. The median gadolinium concentration in the globus pallidus increased from 1.5 to 9.0 μg/g in patients in the contrast group, which is higher than what we had previously observed within this range of GBCA dosing (3), whereas the dose-normalized gadolinium concentrations in other neuroanatomic regions were very similar to those in our previous study.

Localization of Gadolinium within Neuronal Tissues and Assessment of Histologic Changes

Unlike control patients, in whom gadolinium accumulation was not observed (Fig 2, *A*), patients in the contrast group had extensive gadolinium deposits within neuronal tissues detected by means of transmission electron microscopy with energy-dispersive x-ray spectroscopy (Fig 2, *B*). In addition to the absence of gross anatomic differences at autopsy, no gross histologic differences between contrast and

Figure 1

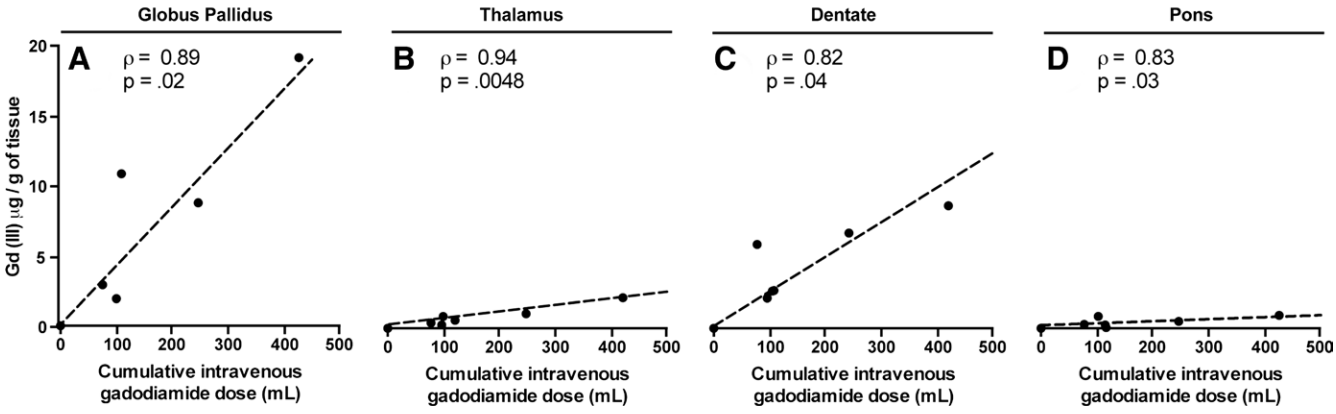

Figure 1: Graphs show gadolinium detection with mass spectrometry of cadaveric tissues. *A–D*, Changes in gadolinium ion signal intensity detected with mass spectrometry plotted against cumulative intravenous gadolinium exposure for each neuroanatomic area. Strength of association between gadolinium ion signal intensity and dose is shown with Spearman rank correlation coefficient (ρ) and associated *P* value.

Figure 2

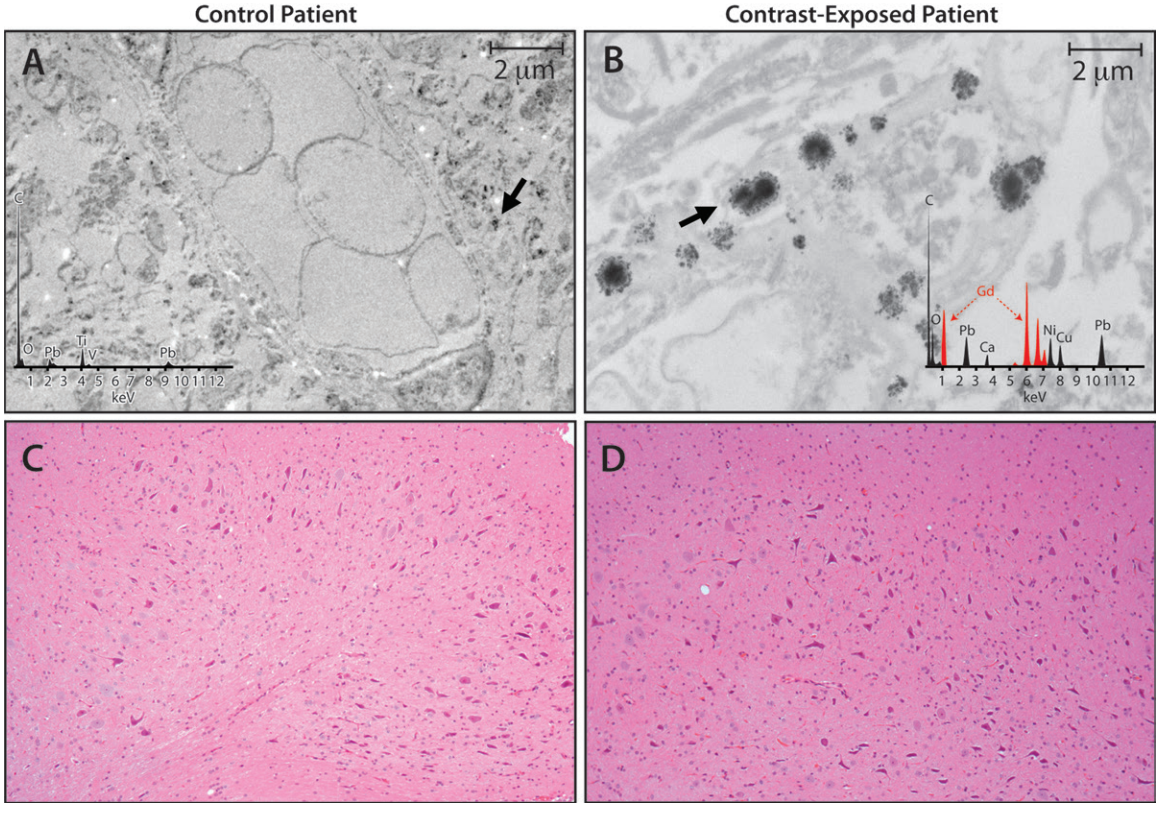

Figure 2: Tissue localization and cellular response to gadolinium deposition. *A, B,* Micrographs from transmission electron microscopy (0.2% lead citrate stain; original magnification, ×10 000) show cellular localization of gadolinium in dentate nuclei tissue samples from, *A,* control patient 7 and, *B,* gadolinium-exposed patient 1. X-ray spectra are shown in inset of each respective panel for selected electron-dense foci (arrows); gadolinium peaks in spectra are indicated by red overlay. *C* = carbon, *Ca* = calcium, *Cs* = cesium, *Cu* = copper, *Gd* = gadolinium, *Ni* = nickel, *O* = oxygen, *Os* = osmium, *Pb* = lead, *Ti* = titanium, *V* = vanadium. *C, D,* Photomicrographs from light microscopy (hematoxylin-eosin stain; original magnification, ×100) of dentate nuclei samples from, *C,* control patient 7 and, *D,* gadolinium-exposed patient 1.

Figure 3

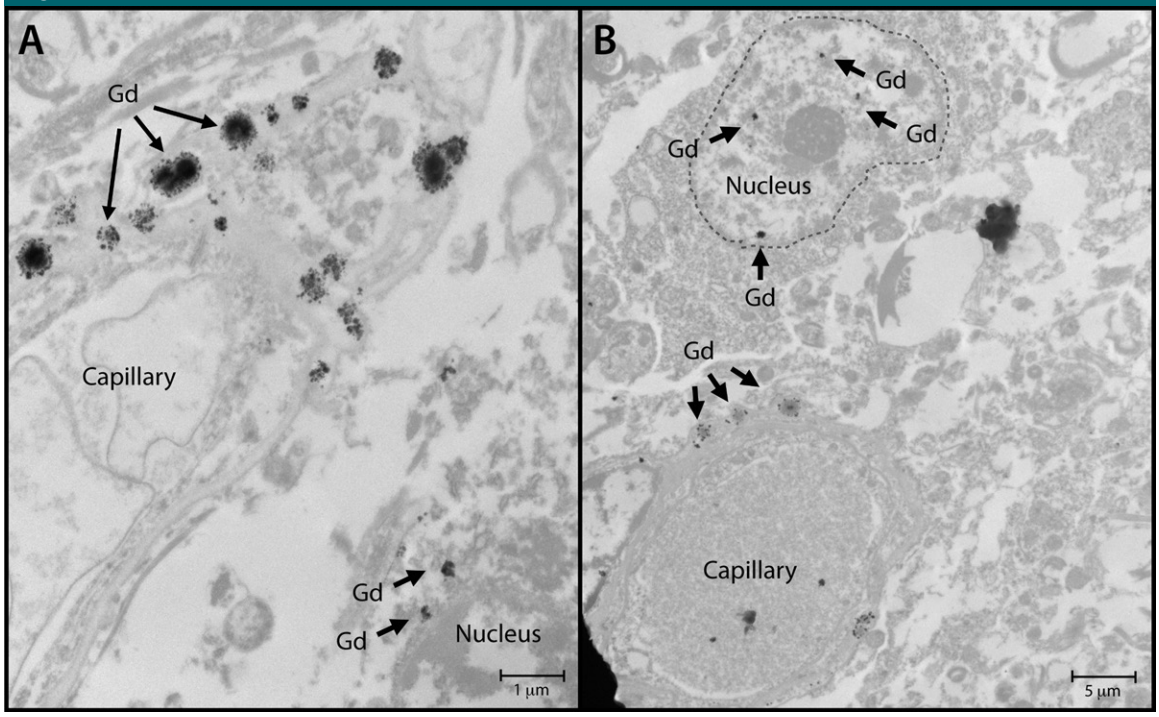

Figure 3: Nuclear localization of gadolinium *(Gd)* deposits. Images from transmission electron microscopy (0.2% lead citrate stain) show cellular localization of gadolinium in dentate nuclei tissue samples from, *A,* gadolinium-exposed patient 1 and, *B,* gadolinium-exposed patient 5 at 2000–10 000-fold magnification. X-ray spectra were collected for selected electron-dense foci (arrows) to verify their identity.

control groups were noted in hematoxylin-eosin–stained samples to suggest cellular injury from gadolinium deposition (Fig 2, *C*, 2, *D*). Although many of the gadolinium deposits were clustered in foci within the endothelial wall, a smaller fraction was found on wider-field views to be in small electron-dense deposits within the neuronal tissue interstitium (Fig 3). In two patient samples, gadolinium deposits were identified within the nucleus of a neuronal cell (Fig 3).

Discussion

The results of this single-center, retrospective study suggest that neuronal tissue deposition of gadolinium after multiple intravenous GBCA doses demonstrates a statistically significant dose-dependent relationship among patients with normal brain morphologic characteristics and presumably an intact blood-brain barrier. Although the neuronal tissue deposition pattern differs somewhat when compared with that in patients with intracranial abnormalities insofar as the deposits are greatest within the basal ganglia rather than in the dentate nucleus in most patients, similar absolute dose-normalized amounts of gadolinium were detected in normal brain tissues (3). Despite direct evidence of gadolinium deposition in neural tissues, we were unable to detect gadolinium-mediated histologic changes that might suggest cytotoxicity. However, the discovery of gadolinium deposits in the nuclei of neurons merits additional investigation in light of the cytotoxic and genotoxic potential of free lanthanide rare earth metals (7–10).

To date, only three previous single-center studies have directly measured gadolinium concentrations in neural tissues of deceased humans by means of ICP-MS (2–4). Our current findings complement and expand upon earlier investigations of patients with intracranial abnormalities to now show ongoing neural tissue accumulation of gadolinium in the absence of such abnormalities. Because the integrity of the blood-brain barrier may be compromised in patients with intracranial abnormalities, our findings provide more definitive evidence of gadolinium accumulation in nondiseased neuronal tissues across an intact blood-brain barrier. Furthermore, our findings complement findings in studies showing that these deposits form in the absence of severe renal or hepatobiliary dysfunction (2,4,11).

Although the dentate nucleus appears to be the preferential site for deposition in patients with intracranial disease, the basal ganglia accumulated a greater amount of gadolinium in our current cohort of patients with normal brain morphologic characteristics. In the current study, gadolinium deposition in the globus pallidus increased sixfold when compared with deposition rates in patients with intracranial abnormalities, whereas deposition rates in other neuroanatomic regions were

similar between studies. The mechanisms of gadolinium deposition remain poorly understood, but it is clear that gadolinium deposits are highest within neuroanatomic regions that are prone to physiologic and pathologic calcification. This observation could be interpreted as evidence that these neuroanatomic regions have less robust capillary basement membranes or that this deposition is a consequence of localization to areas of the brain that are susceptible to cellular stress. Reports of similar MR signal intensity changes in the dentate and/or deep gray nuclei in patients with multiple sclerosis, neurofibromatosis, hypoparathyroidism, inherited metabolic disorders, and Fahr disease corroborate this theory and may suggest that these areas are uniquely susceptible to mineral or metal deposition or injury (12,13). Furthermore, it remains possible that inflammatory and malignant intracranial processes, even when distant from some of the more gadolinium-avid neuroanatomic locations, may increase the permeability of the blood-brain barrier in these locations. However, the normal pathologic and histologic findings in these brains do not suggest that this is a likely cause of the observed deposition. To that end, it remains equally possible that this deposition is nothing more than a case of physiologic mistaken identity whereby gadolinium is mistaken for calcium, given their similar overall atomic diameter and charge (14). Additional research is needed to better understand the mechanism of deposition and nonuniform deposition within the brain parenchyma.

We identified at least two incidences in separate patients wherein gadolinium deposition appeared to be localized to the nucleus of neuronal cells. This finding raises additional concerns regarding the cytotoxicity of deposited gadolinium and the potential for DNA damage (15,16). Although some metals are fairly labile during the paraformaldehyde fixation process, current evidence suggests that gadolinium deposits are fairly insoluble when these fixation agents are used, diminishing the possibility that this nuclear localization is a manifestation of fixation artifact (17,18). Furthermore, artifact from electrostatic interactions between gadolinium deposits and nucleic acids within the nucleus do not adequately explain this apparent localization owing to the relatively small distances over which these attractive forces operate and the mechanism of charge neutralization of biomolecules by means of counterion condensation (19). Although no clinical phenotype appears to be associated with our patient cohort, the expected physiologic effects and clinical significance of lanthanide metal deposition within neuronal tissues are unknown and merit additional investigation.

Our study has several additional limitations. First, because we limited the gadolinium-exposed patients in this study to those with normal brain pathologic characteristics, no intracranial imaging findings were available; therefore, correlations between changes in T1 signal intensities and tissue gadolinium concentrations in this cohort could not be performed. Second, because only a small number of patients met all study criteria and underwent autopsy, the sample size of our contrast group was too small to analyze with multivariate methods. Third, because the patients in this cohort received only the linear agent gadodiamide, we were unable to confirm whether this deposition manifests in both linear and the more stable macrocyclic gadolinium chelates (10,20). Recent evidence from multiple human and animal studies suggest that use of macrocyclic agents reduces deposition, but the extent and mechanism of this reduction remain incompletely understood at this time (21–26). Fourth, we were unable to determine whether the gadolinium detected in neuronal tissues remained in a chelated state or free ionic form. Current tissue-based assays rely on a destructive extraction method that renders the organic ligand undetectable, precluding detection of this chelate. Newer chromatography-based assays such as hydrophilic interaction liquid chromatography–ICP-MS may provide techniques to properly speciate these deposits (27). Notwithstanding these limitations, future efforts directed toward discerning the chelation state of these gadolinium deposits will be critical to our understanding of the mechanism of and risks associated with tissue deposition.

In conclusion, our findings demonstrate that gadolinium deposition in neuronal tissues occurs even in the absence of intracranial abnormalities among patients exposed to multiple gadolinium-enhanced MR examinations. These findings argue for additional studies to better characterize this phenomenon and clarify the safety of GBCAs.

Acknowledgments: The authors thank Amy M. Bluhm, BS, Trace A. Christensen, BS, Jon E. Charlesworth, BS, and Jeffery L. Salisbury, PhD, for their technical expertise.

Disclosures of Conflicts of Interest: R.J.M. Activities related to the present article: disclosed no relevant relationships. Activities not related to the present article: institution received money for consultancy from GE Healthcare. Other relationships: disclosed no relevant relationships. **J.S.M.** Activities related to the present article: disclosed no relevant relationships. Activities not related to the present article: received grants from GE Healthcare. Other relationships: disclosed no relevant relationships. **D.F.K.** Activities related to the present article: disclosed no relevant relationships. Activities not related to the present article: received fees from GE Healthcare for board participation; received a grant from GE Healthcare. Other relationships: disclosed no relevant relationships. **M.E.J.** Activities related to the present article: disclosed no relevant relationships. Activities not related to the present article: received personal fees from Bracco for participation in a gadolinium symposium. Other relationships: disclosed no relevant relationships. **M.A.P.** disclosed no relevant relationships. **D.L.M.** disclosed no relevant relationships. **E.E.W.** disclosed no relevant relationships. **L.J.E.** disclosed no relevant relationships.

References

1. Kanda T, Ishii K, Kawaguchi H, Kitajima K, Takenaka D. High signal intensity in the dentate nucleus and globus pallidus on unenhanced T1-weighted MR images: relationship with increasing cumulative dose of a gadolinium-based contrast material. Radiology 2014;270(3):834–841.

2. Kanda T, Fukusato T, Matsuda M, et al. Gadolinium-based contrast agent accumulates in the brain even in subjects without severe renal dysfunction: evaluation of autopsy brain specimens with inductively coupled plasma mass spectroscopy. Radiology 2015;276(1):228–232.

3. McDonald RJ, McDonald JS, Kallmes DF, et al. Intracranial gadolinium deposition after

contrast-enhanced MR imaging. Radiology 2015;275(3):772–782.

4. Murata N, Gonzalez-Cuyar LF, Murata K, et al. Macrocyclic and other non-group 1 gadolinium contrast agents deposit low levels of gadolinium in brain and bone tissue: preliminary results from 9 patients with normal renal function. Invest Radiol 2016;51(7):447–453.
5. Levey AS, Bosch JP, Lewis JB, Greene T, Rogers N, Roth D. A more accurate method to estimate glomerular filtration rate from serum creatinine: a new prediction equation. Modification of Diet in Renal Disease Study Group. Ann Intern Med 1999;130(6):461–470.
6. R Development Core Team. R: A language and environment for statistical computing. Vienna, Austria: R Foundation for Statistical Computing, 2012.
7. Ray DE, Cavanagh JB, Nolan CC, Williams SC. Neurotoxic effects of gadopentetate dimeglumine: behavioral disturbance and morphology after intracerebroventricular injection in rats. AJNR Am J Neuroradiol 1996;17(2):365–373.
8. Rogosnitzky M, Branch S. Gadolinium-based contrast agent toxicity: a review of known and proposed mechanisms. Biometals 2016; 29(3):365–376.
9. Caillé JM, Lemanceau B, Bonnemain B. Gadolinium as a contrast agent for NMR. AJNR Am J Neuroradiol 1983;4(5):1041–1042.
10. Tweedle MF. Physicochemical properties of gadoteridol and other magnetic resonance contrast agents. Invest Radiol 1992;27(Suppl 1):S2–S6.
11. Errante Y, Cirimele V, Mallio CA, Di Lazzaro V, Zobel BB, Quattrocchi CC. Progressive increase of T1 signal intensity of the dentate nucleus on unenhanced magnetic resonance images is associated with cumulative doses of intravenously administered gadodiamide in patients with normal renal function, suggesting dechelation. Invest Radiol 2014;49(10):685–690.
12. Ginat DT, Meyers SP. Intracranial lesions with high signal intensity on T1-weighted MR images: differential diagnosis. RadioGraphics 2012;32(2):499–516.
13. Kanda T, Nakai Y, Aoki S, et al. Contribution of metals to brain MR signal intensity: review articles. Jpn J Radiol 2016;34(4):258–266.
14. Bourne GW, Trifaró JM. The gadolinium ion: a potent blocker of calcium channels and catecholamine release from cultured chromaffin cells. Neuroscience 1982;7(7):1615–1622.
15. Rim KT, Koo KH, Park JS. Toxicological evaluations of rare earths and their health impacts to workers: a literature review. Saf Health Work 2013;4(1):12–26.
16. Palmer RJ, Butenhoff JL, Stevens JB. Cytotoxicity of the rare earth metals cerium, lanthanum, and neodymium in vitro: comparisons with cadmium in a pulmonary macrophage primary culture system. Environ Res 1987;43(1):142–156.
17. Hare DJ, George JL, Bray L, et al. The effect of paraformaldehyde fixation and sucrose cryoprotection on metal concentration in murine neurological tissue. J Anal At Spectrom 2014;29(3):565–570.
18. Dugar A, Farley ML, Wang AL, et al. The effect of paraformaldehyde fixation on the delayed gadolinium-enhanced MRI of cartilage (dGEMRIC) measurement. J Orthop Res 2009;27(4):536–539.
19. Manning GS. Electrostatic free energy of the DNA double helix in counterion condensation theory. Biophys Chem 2002;101–102:461–473.
20. Port M, Idée JM, Medina C, Robic C, Sabatou M, Corot C. Efficiency, thermodynamic and kinetic stability of marketed gadolinium chelates and their possible clinical consequences: a critical review. Biometals 2008; 21(4):469–490.
21. Kanda T, Oba H, Toyoda K, Furui S. Macrocyclic gadolinium-based contrast agents do not cause hyperintensity in the dentate nucleus. AJNR Am J Neuroradiol 2016;37(5):E41.
22. Kanda T, Osawa M, Oba H, et al. High signal intensity in dentate nucleus on unenhanced T1-weighted MR images: association with linear versus macrocyclic gadolinium chelate administration. Radiology 2015;275(3):803–809.
23. Radbruch A, Weberling LD, Kieslich PJ, et al. Gadolinium retention in the dentate nucleus and globus pallidus is dependent on the class of contrast agent. Radiology 2015;275(3): 783–791.
24. Radbruch A, Weberling LD, Kieslich PJ, et al. High-signal intensity in the dentate nucleus and globus pallidus on unenhanced T1-weighted images: evaluation of the macrocyclic gadolinium-based contrast agent gadobutrol. Invest Radiol 2015;50(12):805–810.
25. Robert P, Lehericy S, Grand S, et al. T1-weighted hypersignal in the deep cerebellar nuclei after repeated administrations of gadolinium-based contrast agents in healthy rats: difference between linear and macrocyclic agents. Invest Radiol 2015;50(8):473–480.
26. Robert P, Violas X, Grand S, et al. Linear gadolinium-based contrast agents are associated with brain gadolinium retention in healthy rats. Invest Radiol 2016;51(2):73–82.
27. Birka M, Wehe CA, Hachmöller O, Sperling M, Karst U. Tracing gadolinium-based contrast agents from surface water to drinking water by means of speciation analysis. J Chromatogr A 2016;1440:105–111.